Enhancing defect detection with Zernike phase contrast in EUV multilayer blank inspection

Yow-Gwo Wang[a, b], Ryan Miyakawa[a], Weilun Chao[a], Markus Benk[a], Antoine Wojdyla[a], Alex Donoghue[a], David Johnson[a], Kenneth Goldberg[a], Andy Neureuther[a, b], Ted Liang[c] and Patrick Naulleau[a]

[a]Center for X-ray Optics, Lawrence Berkeley National Laboratory, Berkeley, CA, 94720

[b]Department of Electrical Engineering and Computer Sciences, University of California, Berkeley, CA, 94720

[c]Intel Corporation, Santa Clara, CA 95054

ABSTRACT

In this paper, we present an experimental verification of Zernike phase contrast enhanced EUV multilayer (ML) blank defect detection using the SHARP EUV microscope. A programmed defect as small as 0.35 nm in height is detected at focus with signal to noise ratio (SNR) up to 8. Also, a direct comparison of the through-focus image behavior between bright field and Zernike phase contrast for ML defects ranging from 40 nm to 75 nm in width on the substrate is presented. Results show the advantages of using the Zernike phase contrast method even for defects with both phase and absorption components including a native defect. The impact of pupil apodization combined with Zernike phase contrast is also demonstrated, showing improved SNR is due to the stronger reduction of roughness dependent noise than defect signal, confirming our previous simulation results. Finally we directly compare Zernike phase contrast, dark field and bright field microscopes.

Keywords: EUV Mask, Zernike Phase Contrast Microscope, Phase Defect, Mask Inspection, Zoneplate

1. INTRODUCTION

For EUV actinic blank inspection, identifying multilayer defects is one of the most critical challenges. Unlike absorber defects, multilayer (ML) defects which are particles on the substrate or defects inside the multilayers predominately vary the optical path of the incoming light while having less impact on the reflectivity of the multilayer. Thus, such defects exhibit limited detectability using conventional bright field microscopy at best focus.

To address this issue, the use of the Zernike phase contrast microscope for EUV actinic blank inspection has been proposed [1, 2]. Zernike phase contrast is capable of detecting phase defects at best focus by enhancing the signal to noise ratio (SNR) through directly interference between the scattered and unscattered light, and the apodization in the pupil plane can further suppress the speckle noise to improve the SNR of the phase defect.

In this paper, experimental results from Zernike phase contrast method using the SEMATECH High-NA Actinic Reticle inspection Program tool (SHARP) are presented. First we present the smallest defect found on a programmed defect test mask using the Zernike phase contrast microscope and the ability to control the through-focus behavior by selection of the phase shifts in the pupil. Then we present data from a variety of defect sizes, and discuss the impact of pupil apodization on signal and noise arising from the mask roughness. Specifically, we show data for the inspection of a native bump defect under various Zernike apodization conditions. Finally, we directly compare the SNR performance from bright field, dark field, and phase contrast miscropes.

2. BACKGROUND

2.1 Optical principle for Zernike phase contrast method

Phase objects do not absorb incident light but rather only change its optical path length. This leads to low sensitivity at focus for conventional bright field microscopy. To overcome this limitation, Zernike phase contrast microscopy [3] utilizes a 90^{o} phase shift and apodization region in the pupil plane to provide extra phase shift to the 0th order

Extreme Ultraviolet (EUV) Lithography VI, edited by Obert R. Wood II, Eric M. Panning,
Proc. of SPIE Vol. 9422, 94221C · © 2015 SPIE · CCC code: 0277-786X/15/$18
doi: 10.1117/12.2087532

(unscattered) light thereby transforming phase modulation into interferometric intensity modulation and also increasing the image contrast by lowering the background intensity. Thus the object sensitivity is much higher at focus. Figure 1 shows the schematic diagrams of both conventional bright field microscopy and Zernike phase contrast microscopy.

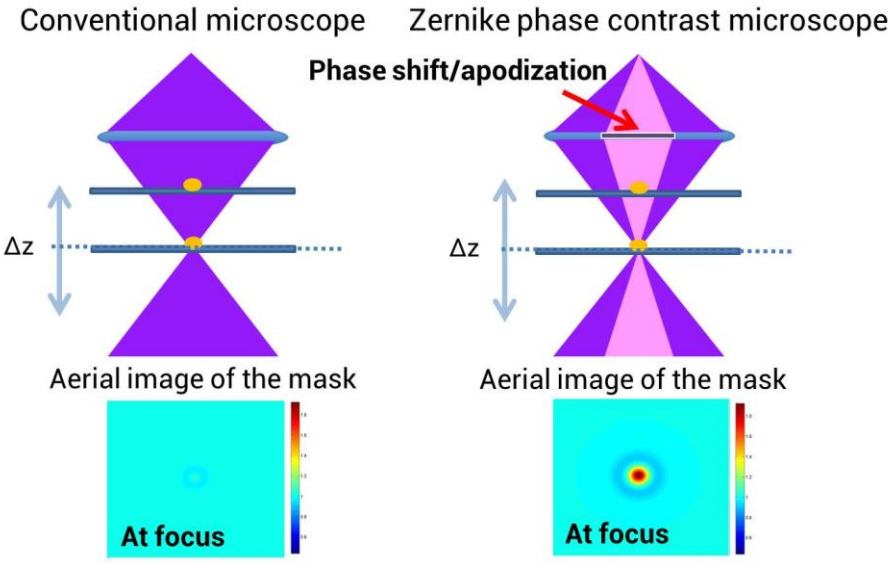

Figure 1. Schematic diagrams of conventional bright field microscope and Zernike phase contrast microscope and their aerial images at focus.

2.2 Defect characteristics: pure phase to attenuated phase defect

Although for convenience we often separately consider phase and absorber defects, in reality true defects are almost always a combination of the two types under inspection [4, 5]. To address this fact, we consider the effectiveness of the Zernike phase contrast method in the presence of such real world "blended" defects. In Figure 2(a) we see the impact of increasing absorption in a conventional microscope through-focus behavior by simulation. Here we use disk illumination with a sigma value of 0.3 and the 4xNA is 0.33. The height of the defects is 1 nm and the FWHM is 60 nm. The difference is that the black line is pure phase and red and blue represent increasing the electric field absorption by defect to 50% and 75%, respectively. Despite this significant change in behavior with defect absorption, the Zernike phase contrast method can still manipulate the phase component of the defect and enhance the defect sensitivity as shown in Figure 2(b).

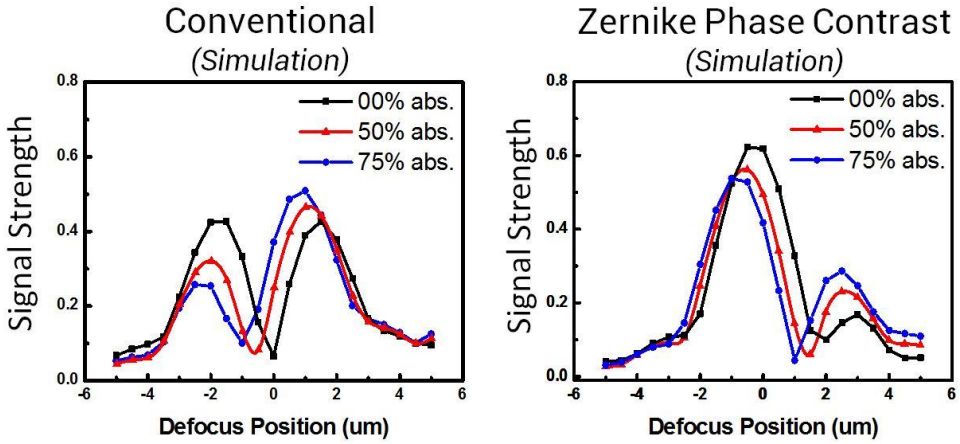

Figure 2. (a) Simulation result of defect signal at different defocus positions using conventional bright field microscope: Pure phase defect (square), phase defect with 50% electric field absorption (triangle), phase defect with 75% electric field absorption (circle). (b) Simulation result of defect signal at different defocus positions using Zernike phase contrast microscope with the same labeling conventions as in (a).

3. EXPERIMENT RESULTS

3.1 Programmed multilayer defect mask sample

The test sample for the experiment is a programmed defect mask [5]. The substrate defects are defined by e-beam lithography using a 48 nm thick hydrogen silsesquioxane (HSQ) resist with a square shape on a quartz substrate. The target defect sizes are from 40 to 75 nm and we consider effectively isolated defects. Figure 3 shows the height and the FWHM of the programmed defects on the multilayer surface as measured by atomic force microscopy (AFM). The surface height is in the range of 0 to 4 nm and the FWHM on the surface ranges from 40 to 60 nm. As previously reported [5], the defects below 50 nm in width on the substrate fall below the AFM sensitivity limit and thus have been omitted from the plot presente ` `

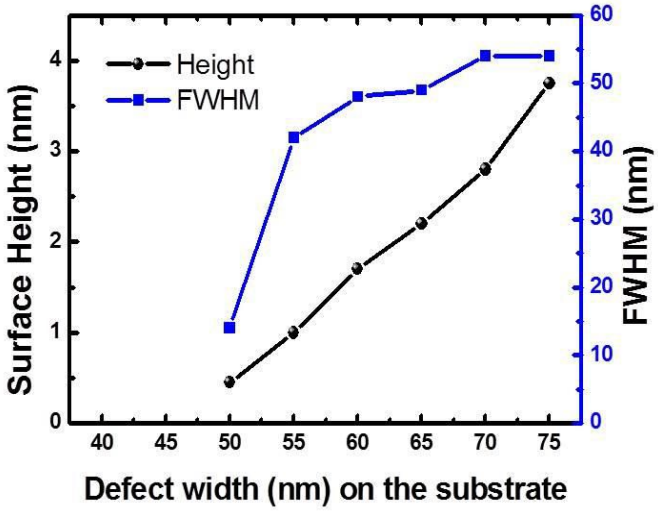

Figure 3. The measured programmed defect height (circle) and FWHM (square) on the surface by AFM. The defect information for defects with a width 40 nm and 45 nm on the substrate are below AFM sensitivity.

3.2 Experiment parameters

The experiment is conducted using the SHARP tool [6], a synchrotron-based EUV microscope for photomask research located at Lawrence Berkeley National Laboratory (LBNL). SHARP's zoneplate architecture greatly facilitates the implementation of the Zernike phase contrast method through the fabrication of specially designed zoneplates. Zone displacement is used to create the phase shift at the desired locations in the pupil and zone duty cycle is used to modulate the diffraction efficiency thereby controlling the apodization.

SEM images of the fabricated Zernike phase shift SHARP zoneplates are shown in Figure 4. The quarter wavelength ($\lambda/4$) displacement in the zone, indicated by the discontinuity of the lines in Figure 4(a), represents a relative 90º phase shift between these two regions in the pupil plane. The variation of duty cycle along the lines from Figure 4(a) to Figure 4(e) shows the intensity modulation from 100% down to 8% for Figure 4(e). The reported intensity apodization values were directly measured in SHARP. Figure 4(f) with zero duty cycle is a dark field zoneplate without phase shifts.

The 4xNA of the bright field and the Zernike phase contrast zoneplates is 0.33 whereas the dark field zoneplate is 0.4. The illumination conditions for the experiment are disk illumination with sigma value of 0.3. We consider a focus range of ± 5 um in 500-nm steps.

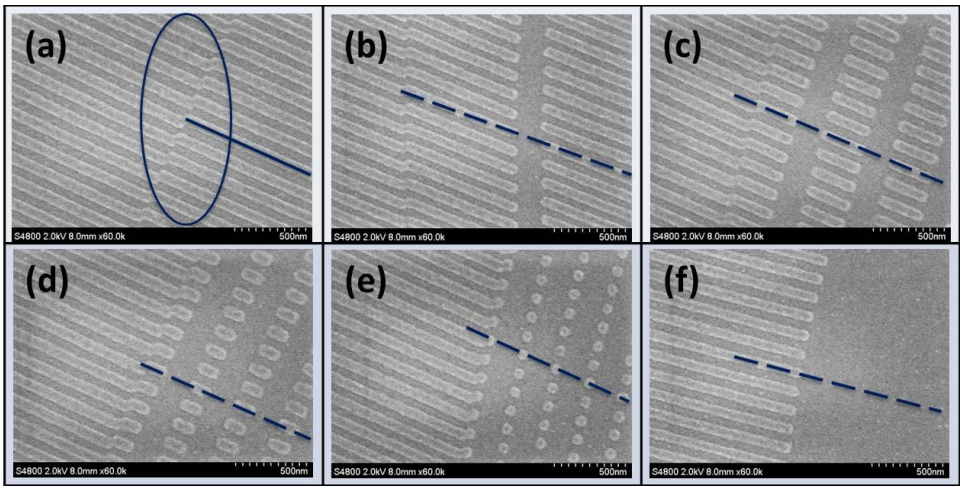

Figure 4. The SEM image of the off-axis Fresnel zoneplates implemented in SHARP: (a) 90 degree phase shift and 100% transmission. (b) 90 degree phase shift and 69% transmission. (c) 90 degree phase shift and 41% transmission. (d) 90 degree phase shift and 20% transmission. (e) 90 degree phase shift and 8% transmission. (f) Dark field.

3.3 Enhanced defect sensitivity using phase contrast method with different phase shifts

Figure 5 shows the complex electric field amplitude and phase from the programmed defect with a width 40 nm on the substrate. The electric field was extracted from through-focus intensity images using a new phase retrieval algorithm described in Ref. [4]. From the complex field of the defect we can readily recover the effective defect height. With only 19º phase shift, the effective height of the 40 nm defect is 0.35 nm. It is interesting to note that this defect was not readily measureable by AFM in the presence of surface roughness noise.

Figure 6 shows the measured through-focus SNR of the 40 nm defect (0.35-nm effective height) using zoneplates with phase shifts of 0º, 45º, and 90º. At 0º (conventional bright field), the through-focus behavior qualitatively matches the expected behavior for a pure phase defect with its minimum sensitivity at focus. On the other hand, at 90º (Zernike phase contrast method), strong signal strength is observed at focus with an SNR of 8. At 45º, the through-focus behavior lies in-between the bright field and phase contrast methods. Note that the minimum SNR occurs away from the best focus position and the peak value on each side of the defocus is different.

These results demonstrate the ability to control the through-focus behavior of multilayer phase defects by tuning the phase shift in the pupil plane. Verifying our previous simulation results [2] that we can use phase shifts other than 90º in order to observe phase and absorber defects with a single scan at focus thereby improving the inspection throughput. More importantly, we can achieve a SNR up to 8 for a phase defect with a height of only 0.35 nm.

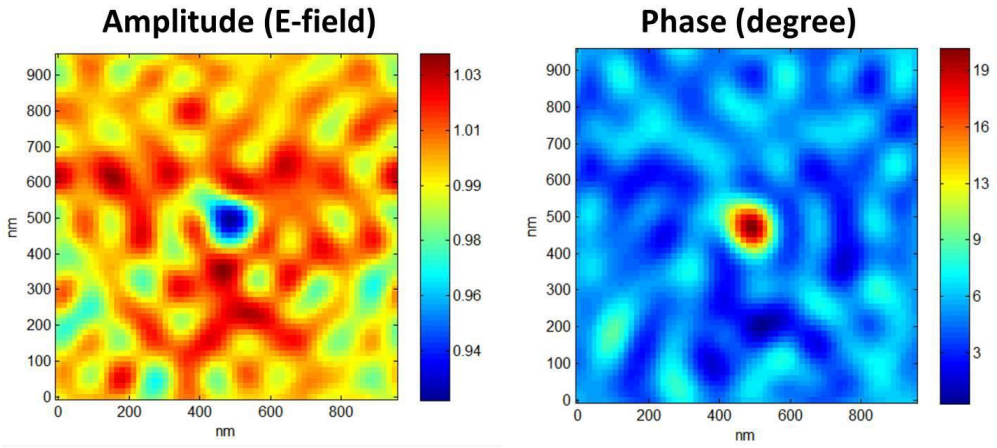

Figure 5. Electric field amplitude and phase extracted from through-focus defect aerial images by phase retrieval algorithm. The phase shift degree can be related to the height of the defect.

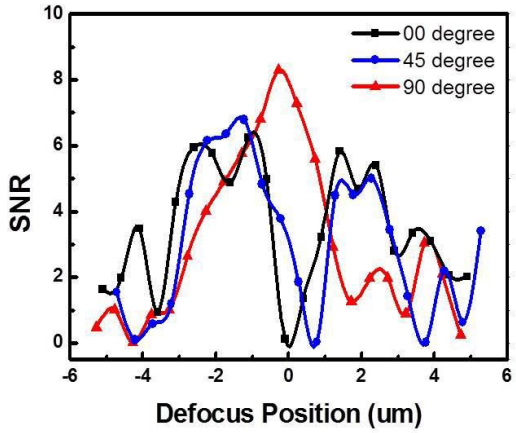

Figure 6. SNR versus positions for the 40 nm defect (0.35 nm effective height) with Zernike phase shift of 0º (square), 45º (circle), 90º (triangle).

3.4 Change in nature of programmed defects with size and inspection implications

Figure 7(a) shows the extracted defect electric field amplitude and phase from SHARP measurements for defect sizes ranging from 40 nm to 75 nm in widths on the substrate. The electric fields show that small defects have little amplitude attenuation but the attenuation grows and transmission decreases nearly linearly with size. This change in nature of the programmed defects with size can also been seen in the measured SNR versus focus for particular defect sizes for bright field inspection. Specifically Figure 7(b) shows SNR versus focus from SHARP measurements for the 40 and 60 nm defects. The 40 nm defect has negligible absorption and SNR is unacceptably low at focus. On the other hand, the 60 nm defect has a more substantial amplitude component and is detectable in focus and has its minimum SNR shifted out of focus.

The Zernike phase contrast microscope can manipulate the phase component of the multilayer phase bumps to provide adequate SNR at focus for both small and large defects. Figure 8 shows the comparison between bright field and Zernike phase contrast measurements from SHARP for 40 nm and 60 nm defects. Both cases indicate that with the phase contrast method, the SNR at focus is better than the bright field situation even for the attenuated phase defect with absorption as shown in Figure 8(b). This result shows that as long as the defect has a significant phase component, the Zernike phase contrast method is effective in enhancing in-focus inspection capabilities with high defect sensitivity. On the other hand, if we lift the restriction of in-focus inspection, the Zernike phase contrast method can outperform bright field by a higher peak SNR at optimum defocus position as shown in Figure 8(b).

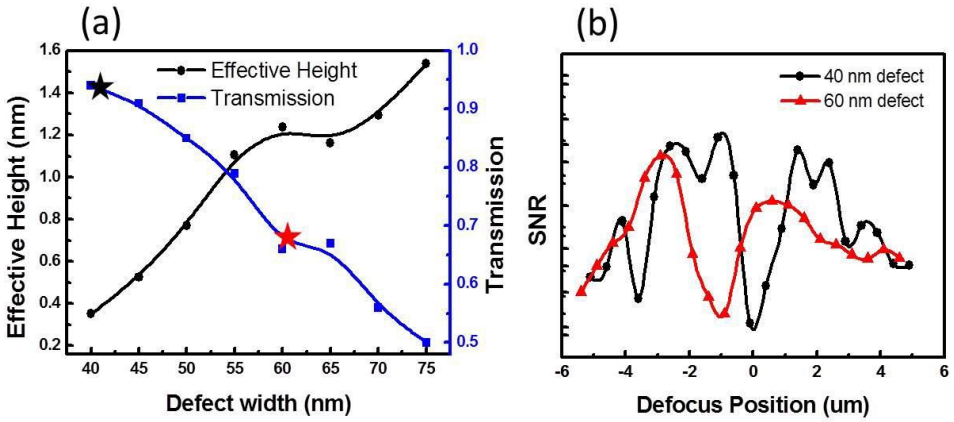

Figure 7. SHARP programmed defect measurements (a) Effective height (circle) and transmission (square) for programmed defects with a width ranging from 40 nm to 75 nm on the substrate. (b) SNR versus positions for the 40 nm defect (0.35 nm effective height, circle) and the 60 nm defect (1.24 nm effective height, triangle) defect from bright field images.

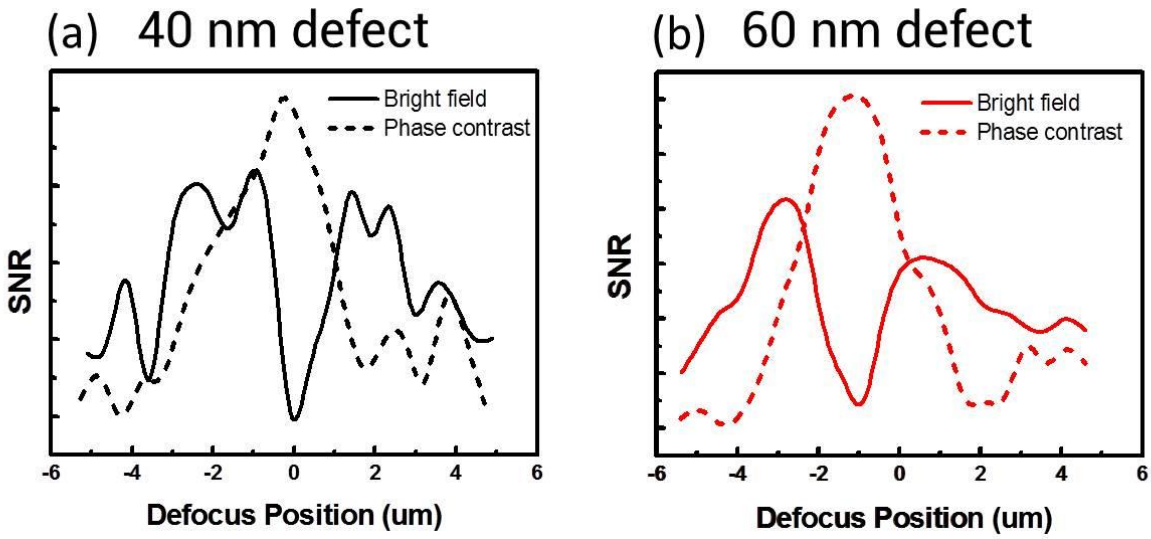

Figure 8. SHARP programmed defect measurements for SNR versus focus for 90 degree Zernike data compared to bright field (a) The 40 nm defect (0.35 nm effective height). (b) The 60 nm defect (1.24 nm effective height).

The SNR at focus for defects with widths ranging from 40 nm to 70 nm is shown in Figure 9 for bright field and 90 degree Zernike SHARP experiments. The behavior depends on the combination of defect height, width, and absorptivity. The height of the defect determines the optical path length which means it determines the amount of phase component of the defect. Detecting this phase with the Zernike method gives a major improvement and provides acceptable SNR for programmed defects below 60 nm. The width of the defect on the surface determines the scattering angle of the defect diffraction. A narrower defect has larger scattering angle and thus not all the photons can be collected by the pupil. Wider defects have smaller scattering angle but more and more of the scattered light passes through the central phase shifted region thus the effect of phase contrast for this portion of the light will be negated [1]. The absorption component of the defect improves the in-focus component for large defects to the point that a nearly similar and adequate SNR is obtained in focus for larger defects. The position of minimum SNR and the asymmetric peak SNR value both are strongly depending on the absorption of the defect and, in fact can be used to recognize the nature of the phase versus amplitude of the defect. Table 1 tabulates a subset of the data in focus SHARP measurement data from Figure 9.

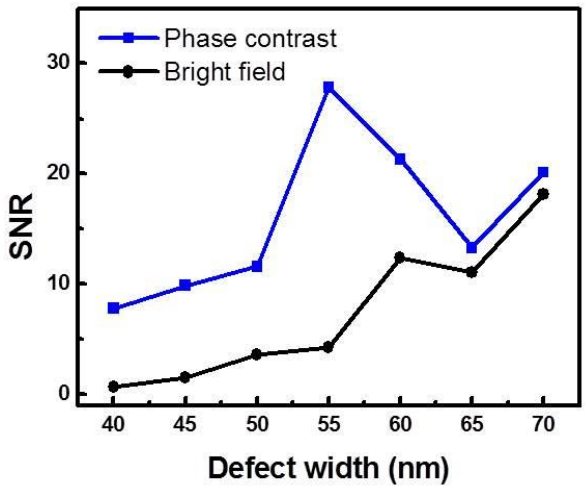

Figure 9. SHARP programmed defect measurements of SNR at focus by bright field (circle) and phase contrast (square) for defects with widths ranging from 40 nm to 70 nm on the substrate.

Table 1. SHARP programmed defect tabular measurements of SNR at focus by bright field and phase contrast.

Method \ Defect	40 nm (H: 0.35 nm)	50 nm (H: 0.77 nm)	60 nm (H: 1.24 nm)	70 nm (H: 1.29 nm)
Bright field	0.70	3.60	12.35	17.12
Phase contrast	7.80	11.60	21.35	20.13
Enhancement	***x11.14***	***x3.22***	***x1.72***	***x1.11***

3.5 The relationship between signal and noise under apodization

In order to further improve the SNR, we apply apodization in the pupil to suppress the low frequency components of the speckle noise from surface roughness while at the same time increasing the contrast of the defect by lowering the DC interferometric reference wave component [2]. For this test we consider a native defect found on the mask with an effective size of 1.23 nm × 120 nm. The effective size was extracted using the phase retrieval method [4] and is shown in Figure 10. We examined five different apodization intensity transmission values: 100%, 69%, 41%, 20%, and 8% for the 90 º Zernike phase shift case. The illumination for this set of data is disk with a sigma value of 0.5.

Table 2 shows the aerial images of the native defect at different defocus positions using different zoneplates on SHARP. The background intensity is normalized to a clear field value of unity in order to compare the defect signal in these different situations. The intensity of the defect from the conventional case (0º/100%) nearly disappears in passing through focus while the results for the phase contrast case (90º/100%) peak through-focus as expected. The signal of the defect relative to the background strongly increases to nearly 3.5 times the background reference, but the speckle noise from the substrate phase roughness is also observed to increase.

The change in the defect signal and phase substrate roughness noise versus apodization level as measured on SHARP is shown in Figure 11. The left hand axis used for both signal and noise and as normalized to their individual levels for the 100% transmission 90 degree Zernike zoneplate. This both signal and noise start from 1 at transmission of 1. As expected, the normalized signal decreases as the transmission decreases. There are two important observations. The first observation is that although the signal decreases with decreasing attenuation the rate of decrease is quite low. The signal level is still about 0.43 when the transmission apodization is only 0.08. This is due to most of the defect diffraction falling in the unattenuated region between the central apodization and the edge of the pupil. The second important observation is that the noise signal is decreasing faster than the signal as the transmission is increased. This is due to the physical characteristics of the phase noise roughness scattering more than the majority of its diffraction at low angles that fall within the apodized pupil region. The mask phase roughness speckle noise decreases a factor of 2 more than the defect signal and results in doubling the SNR from 7 to 14 at an apodization transmission of 0.08.

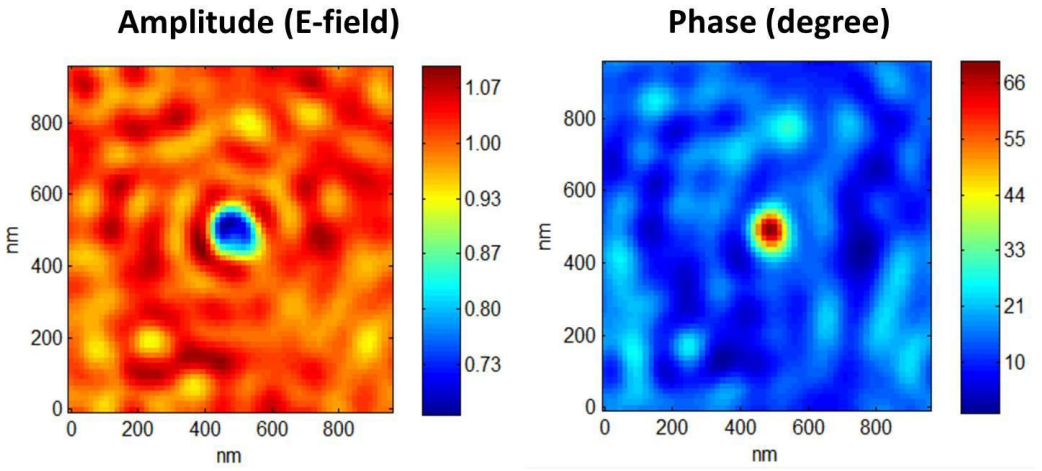

Figure 10. Electric field amplitude and phase for a native defect extracted from SHARP through focus measurements using the phase recovery algorithm. The effective height is 1.23 nm based on the phase of the defect.

Table 2. Aerial images from SHARP for a native defect (1.23 nm effective height) at different defocus position under different pupil conditions.

Method \ Defocus	-4 um	-2 um	0 um	+2 um	+4 um
0°/100%					
90°/100%					
90°/69%					
90°/41%					
90°/20%					
90°/8%					

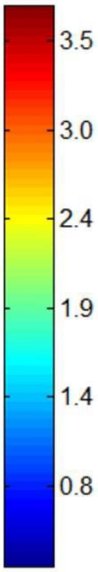

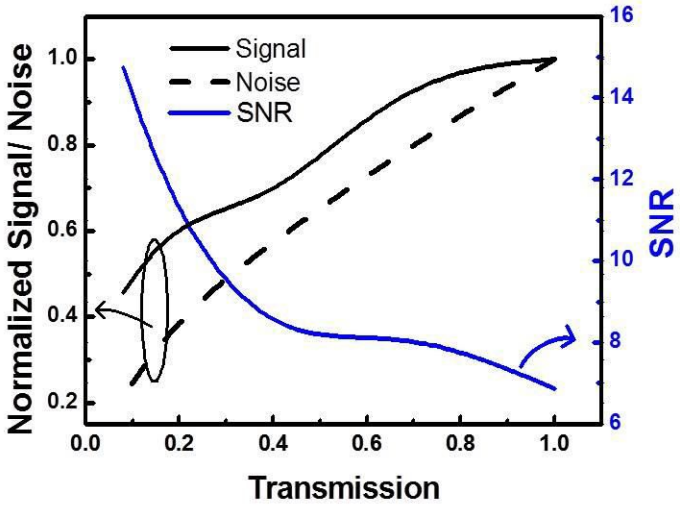

Figure 11. Signal, noise, and SNR for the native defect (1.23 nm effective height) as measured on SHARP at focus under different transmission of the 0.5 sigma apodization in the phase shifted region.

3.6 Bright field vs. Dark field vs. Zernike phase contrast method

To further compare all the possible techniques for actinic blank inspection, we also consider dark field performance by means of SHARP measurements. The programmed defect we use is the 50 nm defect (0.77-nm effective height) with its field shown in the Figure 12. The illumination is a disk with a sigma value of 0.3, the 4xNA for bright field and phase contrast method is 0.33 and the dark field 4xNA is 0.4.

As shown in Figure 13, the through-focus behavior for bright field is still close to the sharp minimum at focus as seen with the 40 nm defect, indicating that this is primarily a phase defect. Again the Zernike phase contrast method shows

the opposite high SNR peak through-focus. Dark field also shows a good SNR peak through-focus. However, the 90° Zernike with 100% transmission has a SNR that is a factor of 1.35 higher at best focus position than the dark field. This improved performance compared to dark field is attributed to the fact that the phase contrast method does not cut off the entire DC component (specular light) like dark field. Rather the phase contrast method uses a fraction of the DC light to constructively interfere with the defect.

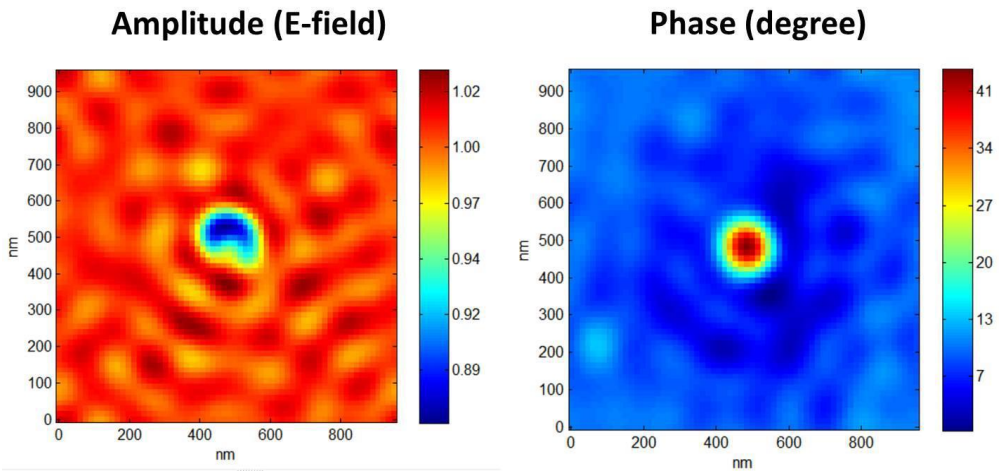

Figure 12. Electric field amplitude and phase for a native defect extracted from SHARP through focus measurements using the phase recovery algorithm. The effective height is 0.77 nm based on the phase of the defect.

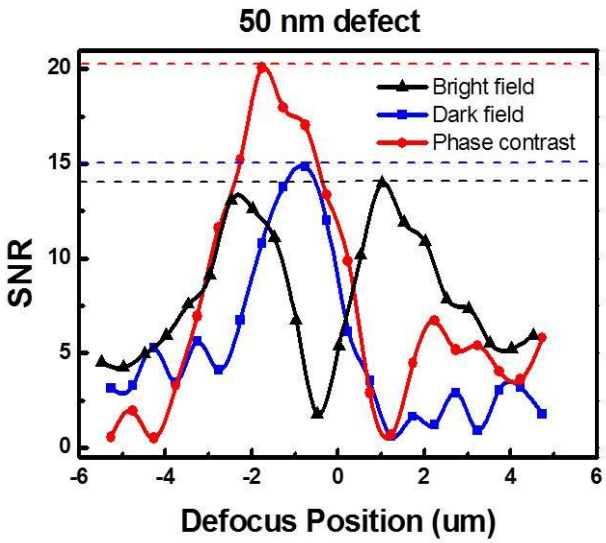

Figure 13. SHARP measurements of the through-focus SNR for the 50 nm defect (0.77 nm effective height) by bright field (triangle), dark field (square), and phase contrast method (circle).

4. CONCLUSION

The SHARP EUV microscope was used to experimentally demonstration of the Zernike phase contrast method for EUV ML blank defect inspection. Zoneplates with central phase shift of 45° and 90° and various level attenuation down to 0.08 intensity transmission were constructed. The experiment results presented here confirm previously presented simulation results [1, 2] of the advantages of Zernike phase contrast inspection. Examples of the effects of blended defects with both phase and absorption show that the absorption causes the problematic null in pure phase defect to shift off-axis. The result demonstrated that phase defects as small as 0.35 nm in height can be detected with a SNR up to 8 at focus. Measurements for a native defect (1.23 nm effective height) using reduced transmission in the phase shifted

region showed that the defect signal decreased much slower than the apodization transmission decrease and also decreased less than the noise. This produced a signal that is 43% of the 100% transmission case with a doubling of the SNR. This improvement is expected to be defect and mask phase noise characteristics dependent as the relative directional scattering in the pupil contributes to these benefits. Measurements for the 50 nm defect (0.77 nm effective height) showed dark field to have good SNR in focus but about a factor of 1.35 lower than for Zernike phase contrast microscopy without apodization.

ACKNOWLEDGMENT

The author would like to thank Intel for their support of the EUV programmed defect mask to conduct the experiment, and the insightful discussion with Rene Claus from UC Berkeley. This research is sponsored by IMPACT+ (Integrated Modeling Process and Computation for Technology). Member companies – Applied Materials, ARM, ASML, Global Foundries, IBM, Intel, KLA-Tencor, Marvell Technology, Mentor Graphics, Panoramic Tech, Photronics, Qualcomm, Samsung, SanDisk and Tokyo Electron.

This work was performed in part at Lawrence Berkeley National Laboratory which is operated under the auspices of the Director, Office of Science, of the U.S. Department of Energy under Contract No. DE-AC02-05CH11231.

REFERENCES

[1] Wang, Y.G., Miyakawa, R., Neureuther, A. and Naulleau, P., "Zernike phase contrast microscope for EUV mask inspection", Proc. SPIE 9048, 904810 (2014).
[2] Wang, Y.G., Miyakawa, R., Chao, W., Goldberg, K., Neureuther, A. and Naulleau, P., "Phase-enhanced defect sensitivity for EUV mask inspection," Proc. SPIE 9235, 92350L (2014).
[3] Zernike, F., "How I discover phase contrast," Science 121, 345-349 (1955).
[4] Claus, R., Wang, Y.G., Benk, M., Wojdyla, A., Donoghue, A., Johnson, D., Goldberg, K., Neureuther, A., Naulleau, P., Waller, L., "Phase measurements of EUV mask defects," Proc. SPIE 9422, 942242 (2015).
[5] Liang, T., Ultanir, E., Zhang, G., Park, S.J., Anderson, E., Gullikson, E., Naulleau, P., Salmassi, F., Mirkarimi, P., Spiller, E. and Baker, S., "Growth and printability of multilayer phase defects on extreme ultraviolet mask blanks," JVSTB 25, 2098 (2007).
[6] Goldberg, K., Benk, M., Wojdyla, A., Mochi, I., Rekawa, S., Allezy, A., Dickinson, M., Cork, C., Chao, W., Zehm, D., Macdougall, J., Naulleau, P. and Rudack, A., "Actinic mask imaging: Recent results and future directions from the SHARP EUV Microscope," Proc. SPIE 9048, 90480Y (2014).